

THEORETICAL AND EXPERIMENTAL STUDY OF THE QUENCHED-DOMAIN MODE

GUNN-EFFECT OSCILLATOR*

Deen D. Khandelwal and Walter R. Curtice
Electron Physics Laboratory
Department of Electrical Engineering
The University of Michigan
Ann Arbor, Michigan

A general large-signal analysis of the quenched-domain mode of Gunn-effect devices has been developed which is applicable to any device without extensive device measurements. Some applications of such an analysis are demonstrated and others are being investigated. The phenomenological model includes such effects as domain formation, domain quenching, domain behavior in the presence of an RF voltage, displacement currents, the voltage dependence of domain width and others.

The basis of the analysis is to obtain an instantaneous current-voltage transfer characteristic for the device. The transfer characteristic consists of an experimental sub-threshold current-voltage characteristic, phenomenological domain formation and quenching processes and stable domain current-voltage characteristic. The displacement current due to the capacitive nature of the domain is then included as well as the bulk displacement current when the domain is not present. This leads to a device equivalent circuit shown in Fig. 1. In this figure, $I_{SD}(V_D)$ is the stable domain current as a function of the domain excess voltage V_D and $C_D(V_D)$ is the domain capacitance. Switches S_1 , S_2 and S_3 are assumed to be open only when there is a domain, when the domain is forming and when the domain is being quenched, respectively.

Using the dynamic domain current-voltage characteristic, a current waveform is evaluated corresponding to the waveform of the device's applied voltage. The voltage includes the fundamental circuit voltage, its harmonics (if present) and the bias voltage. The current waveform thus obtained is

* This work was supported by the Rome Air Development Center under Contract No. F30602-68-C-0043.

Fourier analyzed to obtain the basic results of the large-signal analysis in the form of device admittance plots as a function of the fundamental RF voltage amplitude.

The results reported here pertain to a device 16.2 μm long and having $n_0 = 1.0 \times 10^{15}/\text{cm}^3$ and a low-field conductance of 0.0526 mho.

The threshold and sustaining voltages for the device are 5.265 V and 4.52 V, respectively.

Figures 2 and 3 show the RF conductance and susceptance as a function of the RF voltage for different dc bias voltages and an operating frequency of 10 GHz. It is observed that for very large RF voltages the conductance becomes positive. This occurs because the instantaneous voltage across the device is below its threshold value and in the positive resistance region for a longer period when the RF voltage amplitude is large. Since, for any given bias voltage, there is a minimum value of the RF voltage required for quenching the domain, it is concluded that there is a restricted range of the RF voltage over which a negative conductance is exhibited by a device operating in the quenched-domain mode. It is also observed that when the bias voltage exceeds about 2.4 times the threshold voltage no negative conductance is obtained. A detailed study of the current waveforms has revealed that this results from the conduction current changes as well as excessive domain displacement current. This is a very significant result leading to the conclusion that there exists an upper limit for the bias voltage beyond which the quenched-domain mode is not expected to exist. This also suggests that the circuit-tunable oscillators (at a frequency larger than the transit-time frequency) observed for bias voltages higher than about three times the threshold value cannot be explained by the quenched-domain mode theory.

Figure 4 shows a plot of the power output as a function of the load conductance for different bias voltages and for an operating frequency of 10 GHz. It is observed that for a given bias voltage there exists an optimum load conductance for which maximum power output is obtained and that this optimum load conductance decreases with increasing bias voltage. Explicit results for power output and efficiency for optimum load conditions are shown in Fig. 5.

The behavior of a Gunn-effect device operating in the quenched mode in a single resonant circuit has been analyzed. The electronic tuning characteristic of a device operating in a parallel resonant circuit with

specified circuit parameters R/Q and Q_L is shown in Fig. 6. It is observed that both the power output and the frequency of operation increase with increasing bias voltage until a bias voltage is reached where the quenched-domain mode cannot exist. The difference in the slopes of the power output and efficiency curves is due to the increase in average current with increasing bias voltage which is consistent with our experiments.

To corroborate the theoretical findings, the operating characteristics were measured for the device which has been simulated for the theoretical studies. These characteristics shown in Fig. 7 were obtained by varying the device bias voltage and without altering the circuit conditions. A comparison of Figs. 6 and 7 shows that the device model developed gives results which are in general agreement with the experiments.

Two experimental devices were studied in detail. The first one was 16.2 μm long and showed quenched-mode oscillation over the frequency range 8.5 to 12.5 GHz. The second was 20 μm long and operated in quenched-domain mode in the frequency range 7 to 11 GHz. The quenched-domain mode oscillations were observed for both devices when the bias voltage was in the range $1.1 \text{ V}_{\text{TH}}$ to approximately $2.3 \text{ V}_{\text{TH}}$. Frequency and power output characteristics similar to those of Fig. 7 were always obtained when single frequency oscillations existed. In some cases, decreasing power with increasing bias voltage in higher bias range was observed and under those conditions, substantial second harmonic power was detected.

When bias voltage was increased beyond about 2.3 times the threshold value, noisy power output at many frequencies was obtained for both devices. In certain cases, when proper conditions existed, LSA oscillations were observed for bias voltages greater than about $2.5 \text{ V}_{\text{TH}}$. Whenever the LSA oscillations were obtained, the power output was continuously increasing with increasing bias voltage and the frequency generally decreased with increasing bias voltage. This was observed up to a bias voltage of about 3.5 times the threshold value.

Device admittance has also been evaluated for the oscillating diode with the cartridge, other associated capacitances and the lead inductance and resistance taken into account. Measurements revealed a device capacitance much larger than the low-field capacitance which is in agreement with the calculations. The conductance was used to estimate the RF voltage which was found to be larger than the minimum voltage required for domain quenching.

In conclusion a realistic phenomenological model of the quenched-domain mode of Gunn-effect devices has been described and the supporting experimental results reported. The model is suitable for studying the nonlinear properties of these devices and can be easily extended to other domain modes. The model gives results consistent with experimental operation and reveals the distinguishing features of the quenched-domain mode oscillator.

ACKNOWLEDGMENT

The authors gratefully acknowledge the contributions of Professor G. I. Haddad to this work.



AMERICAN ELECTRONIC LABORATORIES, INC.
P. O. Box 552
Lansdale, Pennsylvania 19446

Products include RF filters, broadband antennas,
solid state components, microwave devices and
microwave integrated circuits.

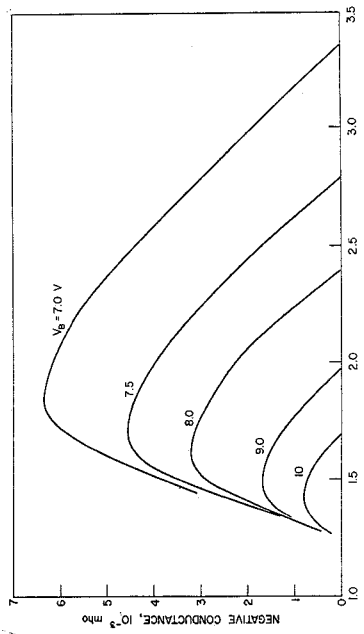


FIG. 2 DEVICE NEGATIVE CONDUCTANCE VS. NORMALIZED RF VOLTAGE V . ($V = V_{RF}/(V_{BLAS} - V_{THRESHOLD})$).

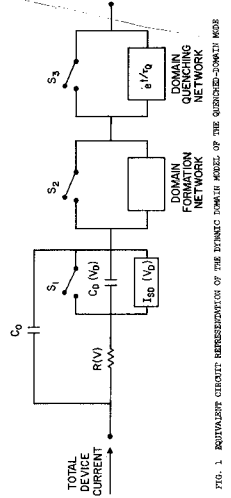


FIG. 1 EQUIVALENT CIRCUIT REPRESENTATION

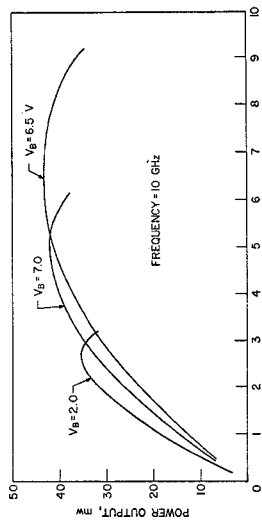
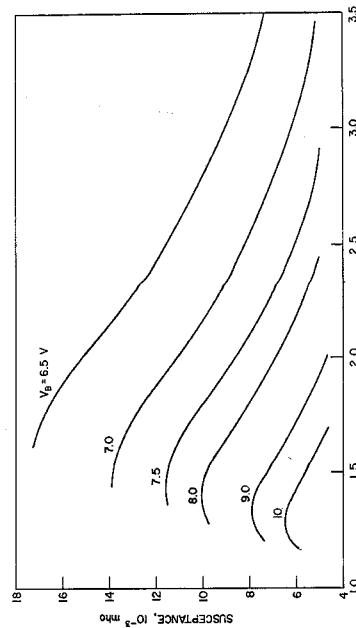


FIG. 4 POWER OUTPUT VS. LOAD CONDUCTANCE FOR DIFFERENT BIAS VOLTMAGES.



NORMALIZED RF VOLTAGE

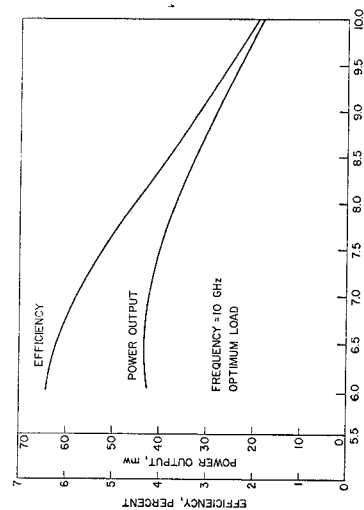


FIG. 5 THEORETICAL OPERATING CHARACTERISTICS OF THE QUENCHED-DOMAIN MODE OSCILLATOR IN A PARALLEL RESONANT CIRCUIT.

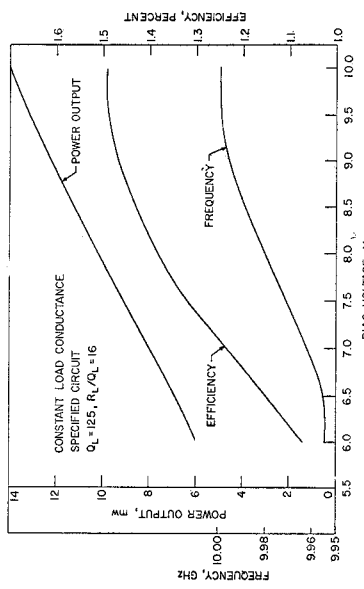


FIG. 6 THEORETICAL OPERATING CHARACTERISTICS OF THE QUENCHED-DOMAIN MODE OSCILLATOR IN A PARALLEL RESONANT CIRCUIT.

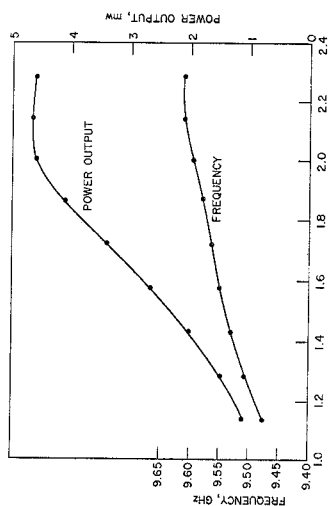


FIG. 7 EXPERIMENTAL OPERATING CHARACTERISTICS OF THE QUENCHED-DOMAIN MODE OSCILLATOR FOR FIXED CIRCUIT CONDITIONS.